Geometry optimization of 7T dual-row transmit arrays

Mikhail Kozlov[1], Roland Müller[1], and Harald Möller[1]
[1]*MPI Leipzig, Leipzig, Saxony, Germany*

Introduction: The most important goals of high field transmit array design are performance, robustness, and safety. A general solution has not yet been found for simultaneous optimization of all these parameters. The performance measures B_{1+v} (B_{1+} averaged over the volume of interest (**VOI**) obtained for a given transmit power), $B_{v\_sar} = B_{1+v}/\sqrt{SAR10g}$ (the safety excitation efficiency), and IB_{1+v} (B_{1+} root-mean-square inhomogeneity), are often subject to trade-offs. A dual-row array design provides more flexibility compared to a single row array. Use of additional degrees of freedom, for example asymmetry in the excitation power for each row (P_{asym}) and a variable phase shift between the array rows (φ_{row}) when excited in a circular polarization mode, together with an optimization using a simple "sweep" procedure, achieves a significant decrease of IB_{1+v}, to as little as 10% calculated over a human brain in some cases [1].

The trade-off between B_{1+v}, B_{v_sar} and IB_{1+v} depends on dual row array geometry, position of a head inside the array, and array tuning condition. The reflected power minimization approach applied to a multi-row array, with no dedicated decoupling network within each row and axially adjacent array rows explicitly decoupled, provides the best $B_{1+v}/\sqrt{P_{transmit}}$ for a given excitation mode [1]. Our numerical simulation goals in this study were: a) to explore trade-off between B_{1+v} and IB_{1+v} for different sweep row overlapping distances and b) to evaluate the robustness of different array geometries upon variation in the head position.

Method: We investigated overlapped dual-row arrays with inductive decoupling networks between all adjacent elements, which were mounted on a cylindrical acrylic former with diameter 280 mm (Fig.1). Each row consisted of 4 radiative elements with angular size of 85° and axial lengths of 110 mm. The loops were made of rectangular copper wire (5 mm × 1 mm). The diameter of the bottom row was increased to 288.4 mm for reliable insulation between overlapped rows. The row overlap distance was varied from 10 mm to 35 mm in steps of 5 mm. The top row was rotated relative to the bottom row by 45°. The loads utilized were the multi-tissue Ansoft human body models, cut in the middle of the torso, with scaling factors: X=0.9, Y=0.9, Z=0.9 (simulating an average head). The head-and-torso model was located at different axial positions so that the distance between the crown of the head and the end of the array was varied from 12 mm to a value yielding a 50mm distance between the crown and array axial center. The simulation approach and post-processing procedures are detailed in [2]. All results were scaled for $P_{transmit}$ of 8 W.

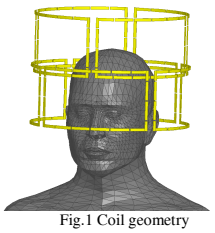
Fig.1 Coil geometry

Results and discussion: The following abbreviations are subsequently used for convenience: "$l \times d$ " denotes an array configuration where l is the row overlap distance in mm, d is the distance between the crown of the head and the end of the array in mm, P_{asym_opt} and φ_{row_opt} are P_{asym} and φ_{row} values yielding the smallest IB_{1+v} for given geometry. Values for two cases are included in Table 1: one obtained for circular polarization (CP) excitation (first three columns) and another one obtained after shimming for minimal inhomogeneity. Each cell contains three values: the first obtained after tuning for a given head position, the second representing the average value for all tuning conditions, and finally the peak-to-peak variation of a given quantity in %. For all geometries, a smooth trade-off between IB_{1+v} and B_{1+v} was obtained. Decreasing IB_{1+v} by a factor of 2 costs about 20% decay in B_{1+v}. However, B_{v_sar} behavior significantly depended on head position. For $d \approx 50$ mm, B_{v_sar} remained almost unaffected, and even increased for geometries with small overlap. For the distance of $d = 12$ mm, there was a significant (~35%) decrease of B_{v_sar}. Thus, for this case the cost of improved inhomogeneity is an increase in SAR10g by as much as a factor of 1.8.

Geometry $l \times d$	*CP* B_{1+v}, μT / μT / %	*CP* IB_{1+v}, % / % / %	*CP* B_{v_sar}, μT/√W/kg /… / %	B_{1+v}, μT / μT / %	IB_{1+v}, % / % / %	B_{v_sar}, μT/√W/kg / … / %	P_{asym_opt}	φ_{row_opt}
10×12	1.20/1.12/20	27/25/15	0.73/0.67/15	1.04/1.04/4	15/15/3	0.54/0.55/4	0	90
10×42	1.45/1.42/8	25/25/23	0.73/0.73/19	1.2/1.17/5	13/13/2	0.65/0.64/5	-15	90
10×57	1.51/1.42/13	28/31/31	0.71/0.65/16	1.25/1.25/3	12/14/24	0.75/0.73/4	-15	80
15×12	1.29/1.19/20	27/25/13	0.73/0.70/13	1.08/1.07/3	15/15/4	0.54/0.55/7	0	90
15×37	1.49/1.45/8	25/25/20	0.73/0.74/16	1.21/1.2/3	13/13/3	0.63/0.63/4	-10	90
15×52	1.56/1.49/11	27/30/20	0.71/0.66/14	1.28/1.28/3	12/13/21	0.73/0.72/4	-10	80
20×12	1.33/1.24/19	26/25/12	0.74/0.72/11	1.15/1.15/4	15/15/7	0.56/0.58/7	-10	90
20×32	1.5/1.47/9	25/24/17	0.74/0.75/12	1.21/1.25/5	13/13/8	0.61/0.64/10	-10	90
20×47	1.59/1.53/9	26/30/18	0.72/0.67/12	1.29/1.31/5	12/13/21	0.72/0.71/3	-10	80
25×12	1.37/1.29/16	26/25/9	0.74/0.73/9	1.16/1.15/2	14/15/5	0.56/0.57/9	-10	90
25×32	1.53/1.51/7	25/25/15	0.74/0.75/13	1.22/1.25/5	13/13/4	0.62/0.63/7	-10	90
25×52	1.6/1.57/6	26/28/16	0.73/0.69/11	1.30/1.31/4	12/13/20	0.70/0.69/3	-10	80
30×12	1.4/1.3/18	26/25/10	0.75/0.73/9	1.17/1.17/5	14/14/8	0.56/0.59/9	-10	90
30×32	1.56/1.53/8	24/24/16	0.75/0.75/13	1.28/1.26/3	13/13/6	0.64/0.64/7	-10	80
30×52	1.61/1.58/7	26/28/17	0.73/0.69/11	1.29/1.32/7	12/13/23	0.71/0.70/3	-10	80
35×12	1.43/1.37/21	26/25/13	0.75/0.74/9	1.19/1.23/10	14/15/12	0.57/0.59/6	-15	90
35×32	1.58/1.57/10	24/25/19	0.72/0.73/16	1.29/1.29/6	13/13/12	0.66/0.66/12	-15	80
35×52	1.62/1.59/10	26/29/19	0.73/0.68/13	1.29/1.32/7	12/12/24	0.72/0.71/4	-15	80

Conclusion: Different tuning conditions resulted in larger peak-to-peak variation for CP excitation than for excitations that minimized IB_{1+v}. For these excitations IB_{1+v} decreased from 15% to 12% when the head was located in middle of the coil. This position is clearly preferable for keeping the safety excitation efficiency unaffected. For an overlapping dual row array with four elements in each row designed for full-brain coverage, a small overlap is preferable. Current values through different parts of one radiative element with axial lengths of 110 mm showed essential variation. Thus, increasing this length was not a solution to maintain the overall coil length for increased overlapping. The current investigation is limited regarding sensitivity analysis for variation of overlapping because the total axial length of the coil was decreased increased overlap.

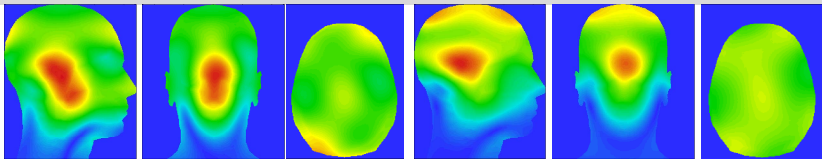
Fig.2 B_{1+} slices rescaled to max value from Table I: left geometry 10×12, right 10x57

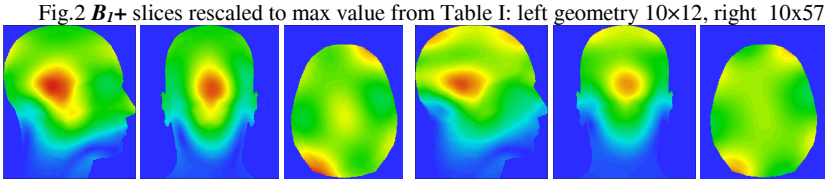
Fig.3 B_{1+} slices rescaled to max value from Table I: left geometry 35x12, right 35x52

[1] M. Kozlov, R. Turner, Proceedings of APMC 2012, Kaohsiung, Taiwan, pp. 815-817. [2] M. Kozlov, R. Turner, Proceedings of the 43rd European Microwave Conference, Nuremberg, Germany, 2013, pp. 708-711.